

## Evidence of Stabilization in the Z-Pinch

U. Shumlak, R. P. Golingo, and B. A. Nelson

*University of Washington, Aerospace and Energetics Research Program, Seattle, Washington 98195-2250*

D. J. Den Hartog\*

*Sterling Scientific, Inc., Madison, Wisconsin*

(Received 11 June 2001; published 29 October 2001)

Theoretical studies have predicted that the Z-pinch can be stabilized with a sufficiently sheared axial flow [U. Shumlak and C. W. Hartman, *Phys. Rev. Lett.* **75**, 3285 (1995)]. A Z-pinch experiment is designed to generate a plasma which contains a large axial flow. Magnetic fluctuations and velocity profiles in the plasma pinch are measured. Experimental results show a stable period which is over 700 times the expected instability growth time in a static Z-pinch. The experimentally measured axial velocity shear is greater than the theoretical threshold during the stable period and approximately zero afterwards when the magnetic mode fluctuations are high.

DOI: 10.1103/PhysRevLett.87.205005

PACS numbers: 52.58.Lq, 52.30.-q, 52.35.Py

The Z-pinch plasma configuration has been studied since the beginning of the pursuit of magnetic plasma confinement fusion [1–3]. The Z-pinch was largely abandoned as a magnetic confinement configuration due to violent magnetohydrodynamic (MHD) instabilities (gross  $m = 0$  “sausage” and  $m = 1$  “kink” modes) demonstrated both theoretically and experimentally [4]. However, experiments have generated Z-pinch plasmas with inherent axial plasma flows exhibiting stable confinement for times much longer than the predicted growth times [5,6]. A stable, high-density Z-pinch configuration would have profound implications for magnetic confinement thermonuclear fusion [7–9].

Theoretical studies have demonstrated that the Z-pinch can be stabilized with a sufficiently sheared axial flow [10]. Experimental results presented here show a stable period which is over 700 times the expected instability growth time in a static Z-pinch. The experimentally measured axial velocity shear is greater than the theoretical threshold during the stable period and approximately zero afterwards when the magnetic mode fluctuations are high. The correlation of the experimental stability data with the plasma flow measurements is consistent with the shear flow stabilization theory presented in Ref. [10]. However, at this point causality cannot be determined.

The role of plasma flow on the MHD instabilities in a Z-pinch has been examined theoretically using linear stability analysis [10,11]. The fundamental result from both of these studies is the Z-pinch can be stabilized by applying a sheared axial flow though the required magnitude of the plasma flow differs for these two studies. Reference [10] concludes that an axial plasma flow with a linear shear of  $v_z/a > 0.1kV_A$  is required for stability of the  $m = 1$  mode where  $k$  is the axial wave number. Reference [11] concludes that an axial plasma flow of  $v_z > 2 - 4V_A$  is required for stability of all modes with  $ka = 10$ . Both of these results are for a conducting wall placed far enough

from the plasma boundary that it has no effect. Nonlinear results for the  $m = 0$  mode are presented in Fig. 1. The results are generated using Mach2 [12,13], a time-dependent, resistive MHD code. An equilibrium is initialized with a sheared axial plasma flow and an axially periodic density perturbation. The figure shows the pressure contours for the case of (a) no flow and (b)  $v_z/a = 0.2kV_A$  at the same simulation time. Figure 1(a) shows a well-developed  $m = 0$  instability in a static Z-pinch plasma. Figure 1(b) shows a substantially less developed  $m = 0$  instability in a Z-pinch plasma with a sheared axial flow.

The ZaP (Z-pinch) experiment at the University of Washington has been used to investigate the effect of plasma flow on the stability of a Z-pinch. The experiment is designed to generate a Z-pinch plasma which contains a large axial flow. The experimental device is depicted in Fig. 2. The flow Z-pinch configuration is generated by using a coaxial accelerator to initiate the hydrogen plasma

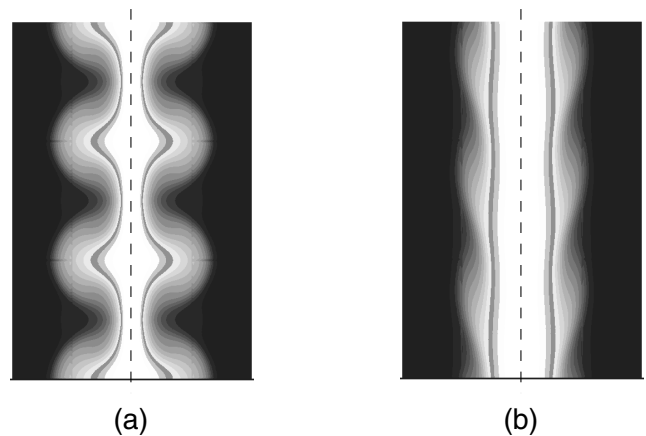


FIG. 1. Nonlinear simulation results showing the pressure contours in a Z-pinch at the same simulation time (a) for the developed  $m = 0$  mode with no equilibrium axial flow and (b) for the stabilized  $m = 0$  mode with  $v_z/a = 0.2kV_A$ .

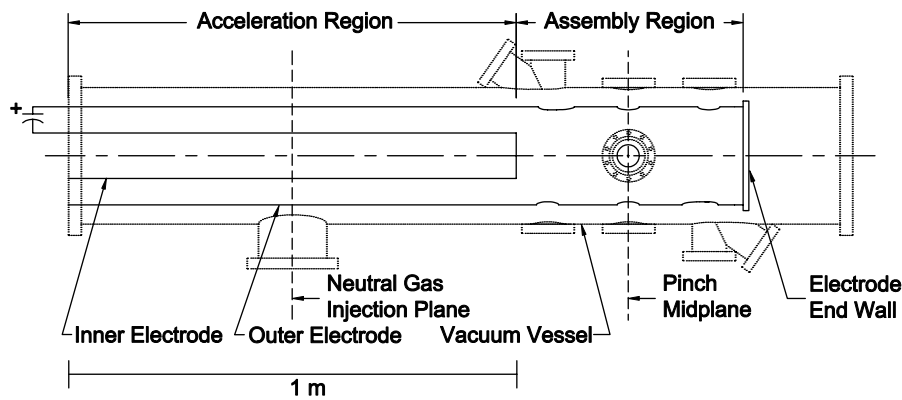


FIG. 2. Side view drawing of the ZaP experiment showing the relevant features. The solid lines indicate the electrodes and the dotted lines indicate the vacuum vessel. The top and bottom ports in the assembly region are used for spectroscopy, and the side ports are used for obtaining images from the fast framing camera and measuring density.

from puff injected neutral gas and to accelerate the plasma axially in the “acceleration region.” When the plasma reaches the end of the inner electrode of the accelerator, the plasma assembles along the axis in the “assembly region.” The plasma in contact with the outer electrode continues to move axially until it reaches the electrode end wall where the plasma moves radially inward to complete the pinch formation. The axial plasma flow is maintained in the pinch by inertia. Plasma is accelerated and incorporated into the pinch continually by current in the acceleration region. The plasma accelerator operates in a “quasi-steady-state” mode that has been described previously [14].

The Z-pinch plasma has a 50 cm length and an approximately 1 cm radius when assembled. The peak plasma current supplied from a 46 kJ capacitor bank is 275 kA and has a quarter cycle time of 30  $\mu\text{sec}$ . The experimental measurements presented in this paper are obtained at the pinch midplane as identified in Fig. 2.

The electron number density in the plasma pinch is determined from a two chord He-Ne heterodyne quadrature interferometer. One chord traverses the plasma midplane along the geometric diameter, and a second chord is parallel to and 2 cm above the first chord. The plasma density is assumed to have spatially uniform values outside and inside the pinch radius determined from optical emission and spectroscopic data. The plasma electron number density is determined to be  $10^{16}$ – $10^{17}$   $\text{cm}^{-3}$  inside the pinch.

The magnetic field measured at the outer electrode at the pinch midplane with surface mounted magnetic probes is 0.15–0.25 T. The magnetic field at the pinch radius is then 1.5–2.5 T assuming no plasma current outside of the pinch radius. The total plasma temperature ( $T_e + T_i$ ) is estimated from force balance to be 150–200 eV. The ion temperature is calculated from Doppler broadening of impurity lines to be 50–80 eV.

Eight surface magnetic probes are equally spaced around the azimuth at the pinch midplane. The probes measure the azimuthal magnetic field at the surface of the outer electrode. Data from these probes are Fourier analyzed to

determine the time-dependent evolution of the low order azimuthal modes ( $m = 1, 2, 3$ ). Figure 3 shows the time evolution of the  $m = 1$  and  $m = 2$  Fourier modes of the magnetic field. The average magnetic field  $B_0(t)$  of all eight probes is used to normalize the Fourier mode data at the pinch midplane. The  $m = 3$  mode (not shown in the figure) is also analyzed and is lower than the  $m = 2$  level at all times. The figure also shows the evolution of the total plasma current for reference.

The plasma arrives at the pinch midplane at approximately 18  $\mu\text{sec}$ . Magnetic mode fluctuation data before this time can be ignored and are caused by small signal noise which is amplified in the normalization procedure. After the pinch has formed the initially large fluctuation levels for both  $m = 1$  and  $m = 2$  change character for approximately 17  $\mu\text{sec}$ . The change in character is identified by lower levels and decreased frequency. The fluctuation levels then again change character, increase in magnitude and frequency, and remain until the end of the plasma pulse.

Optical emission images of the pinch midplane are obtained with a fast framing camera every 1  $\mu\text{sec}$ . The images show a stable pinch that becomes unstable to a kink

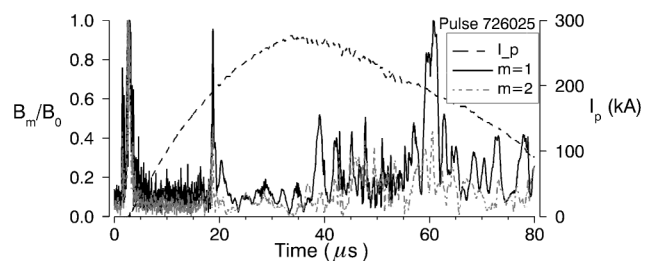


FIG. 3. Time evolution of Fourier components of the magnetic field fluctuation at the pinch midplane for  $m = 1$  and  $m = 2$  showing the quiescent period from 21 to 38  $\mu\text{sec}$ . The values are normalized to the average magnetic field value at the pinch midplane. The evolution of the total plasma current (dashed curve) is included for reference.

mode. The timing of the stable period corresponds to the stable time shown in the magnetic data.

Plasma flow velocity profiles are determined by measuring the Doppler shift of plasma impurity lines using a 0.5 m imaging spectrometer with an intensified charge-coupled device (ICCD) detector. The ICCD camera is set to a gating time of 1  $\mu\text{sec}$  and the trigger time is varied between plasma pulses. The spectrometer images 20 spatial chords through the plasma onto the ICCD camera using telecentric viewing telescopes [15]. The telescopes are connected to the spectrometer with a fiber bundle composed of twenty fused silica fibers. The chords image 20 points spaced 1.24 mm apart along a diameter through the pinch. Optical access to the midplane is provided through radial viewports and oblique viewports positioned at a 35° angle to the plasma column, as shown in Fig. 2.

Doppler shifts are calculated by viewing the plasma through the radial viewport to locate the unshifted impurity line and then viewing the plasma through the oblique viewport. The oblique view has a directional component along the axis and, therefore, is sensitive to Doppler shifts from axial flows. Figure 4 shows the output from the ICCD spectrometer tuned to the C-III line at 229.7 nm and viewing the plasma through the oblique viewport. The trigger time for the ICCD is 30  $\mu\text{sec}$  which is during the quiescent period. (This pulse is the same presented in Fig. 3.) The data show a shift of the C-III line being emitted from the chords of the inner core of the pinch and a lesser shift of the line being emitted from the edge of the pinch.

The data are deconvolved to resolve the spatial dependence of the Doppler shift of the impurity line. The raw data are corrected to remove instrument distortions and binned into 20 nonoverlapping spatial chords. The binned data are deconvolved by assuming the plasma is uniform within 10 concentric shells. The spectral line shapes at each chord location are fit with Gaussians modified by the

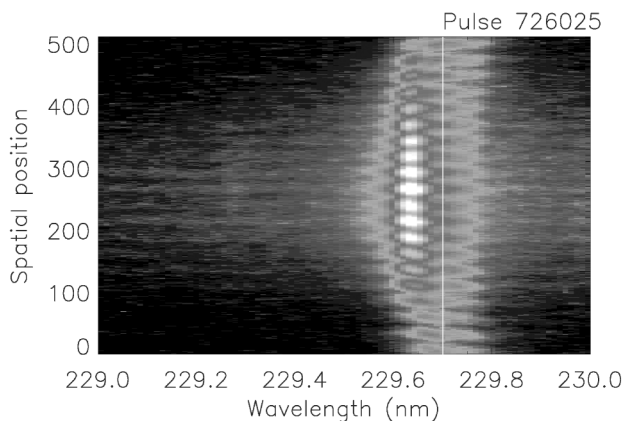


FIG. 4. Chord-integrated C-III line (229.7 nm) emission at 30  $\mu\text{sec}$  with a 1  $\mu\text{sec}$  gate obtained with the ICCD spectrometer showing the Doppler shift of the impurity line in the core of the pinch and a smaller shift towards the edge of the plasma. The solid line is positioned at 229.7 nm for reference. (The peak signal to noise ratio of the lowest intensity chord is 15.5.)

instrument function and account for the chord-integrated view through outer shells. The procedure is repeated beginning from each edge of the plasma. Fit parameters are the location of the plasma edge, the plasma axis location, and the emissivity, Doppler shift, and Doppler width of the emitted light at each chord location. The deconvolved velocity profile for the data shown in Fig. 4 is presented in Fig. 5. The lack of symmetry in the fitted profiles indicates a lack of symmetry in this plasma pulse. The symmetry of the deconvolved fit is sensitive to the plasma axis location. The emissivity profile (not shown) indicates the plasma has a characteristic pinch radius of approximately 1 cm and is centered in the horizontal plane with respect to the experimental geometry. The velocity profile in Fig. 5 shows a large axial velocity in the inner core of the pinch of  $10^5$  m/s and a lower value of  $4 \times 10^4$  m/s towards the edge of the pinch.

After the quiescent time the plasma flow velocity is significantly reduced. Figure 6 shows the ICCD output for the same setup as previous with a trigger time of 38  $\mu\text{sec}$  which is after the quiescent period and when the magnetic mode activity is high. The spectra for all of the spatial locations are centered on the 229.7 nm reference line in the figure. A maximum limit to the velocity is determined by fitting the chord integrated data with two Gaussian functions having equal widths which overestimates the velocity. (An accurate deconvolution is not possible without simultaneous data to identify the edge and center of the plasma.) The peaks are broader indicating random plasma motion and plasma heating due to flow stagnation on the electrode end wall, identified in Fig. 2. At a velocity of  $10^5$  m/s the plasma flows through the 50 cm assembly region in 5  $\mu\text{sec}$ .

The experimental data from the plasma optical emission and surface magnetic probes indicate the plasma, which is initially unstable during assembly, forms a stable plasma

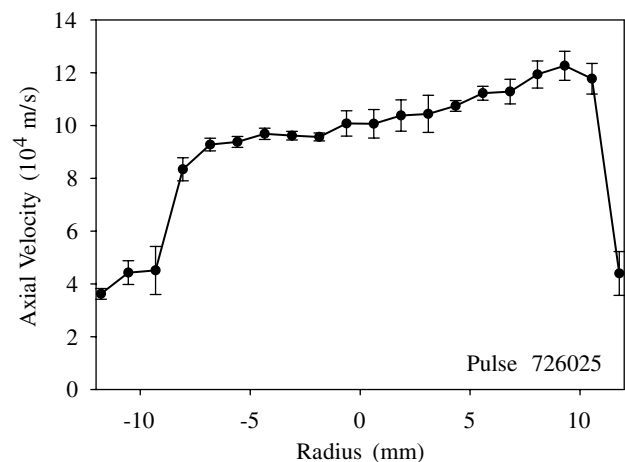


FIG. 5. Plasma axial velocity profile based on the C-III line at 229.7 nm as a function of geometric radius showing a large axial velocity in the inner core of the pinch and a shear towards the edge of the pinch.

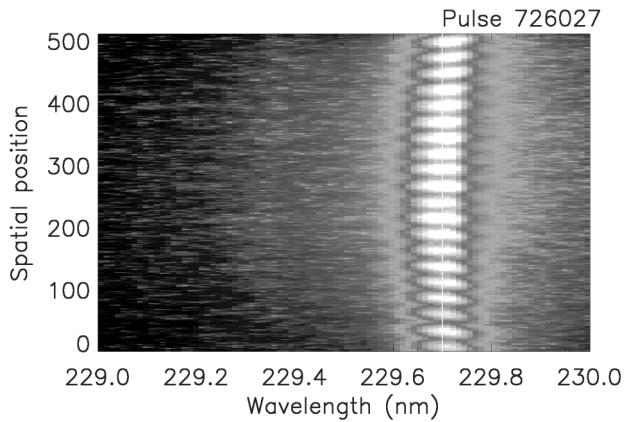


FIG. 6. Chord-integrated C-III line (229.7 nm) emission at 38  $\mu\text{sec}$  with a 1  $\mu\text{sec}$  gate obtained with the ICCD spectrometer showing a negligible Doppler shift of the impurity line. The solid line is positioned at 229.7 nm for reference.

pinch. The plasma remains stable during a 15–20  $\mu\text{sec}$  quiescent period. During the quiescent period the plasma flow is organized into a profile that has a large shear of the axial velocity and is maximum close to the plasma edge. After the quiescent period the plasma becomes unstable as evidenced by an increase in magnetic fluctuation levels and a disappearance of the pinch from the field of view of the optical camera. After the quiescent period the flow velocity is mostly uniform with a maximum considerably less than during the quiescent period.

The measured axial flow shear can be compared to the required threshold predicted by linear theory. The magnetic field at the outer electrode is measured to be 0.18 T for a magnetic field value at the characteristic pinch radius  $B_a = 1.8$  T assuming zero plasma current density for  $r > a$ . The electron number density in the pinch is measured to be  $n = 9 \times 10^{16} \text{ cm}^{-3}$ . The Alfvén velocity is  $V_A = B_a / \sqrt{\mu_0 M_i n} = 1.3 \times 10^5 \text{ m/s}$ , where  $M_i$  is the mass of a hydrogen ion. The theoretical growth rates for a static plasma are approximately  $kV_A$  for the  $m = 1$  mode and  $V_A/a$  for the  $m = 0$  mode. For a typical value of  $ka = \pi$  the shortest growth time would be 24 nsec for a static Z-pinch plasma with the magnetic field strength, density, and radius measured on the ZaP experiment. The required axial velocity shear for stability according to the shear flow stabilization theory presented in Ref. [10] is  $4.2 \times 10^6 \text{ s}^{-1}$ .

The experimental results show a stable period of 17  $\mu\text{sec}$  which is over 700 growth times. The experimentally measured axial velocity shear is  $1.9 \times 10^7 \text{ s}^{-1}$  during the stable period and approximately zero afterwards when the magnetic mode fluctuations are high. The correlation of the experimental stability data with the plasma flow measurements is consistent with the shear flow stabilization theory presented in Ref. [10].

The presence of a sheared axial plasma velocity is coincident with low magnetic fluctuations; however, it has not been determined that the decrease in the plasma velocity shear leads to the increase in the magnetic fluctuations. Therefore, at this point causality cannot be determined.

Axial plasma velocity profiles with a radial shear have been measured in a Z-pinch plasma. Significant reductions in the magnetic fluctuations are coincident with the presence of the sheared sub-Alfvénic plasma flows. The experimental evidence is consistent with the theory that gross MHD modes can be stabilized with sufficiently sheared axial plasma flow. Nonlinear simulations also support this theory. The sheared flow stabilization of the disruption modes in Z-pinch has important implications for the flow-through Z-pinch and other magnetic confinement configurations.

This work is supported through a grant from the Department of Energy. The authors wish to acknowledge E. A. Crawford and T. R. Jarboe for valuable discussions.

---

\*Present address: Department of Physics, University of Wisconsin-Madison, 1150 University Avenue, Madison, Wisconsin 53706.

- [1] W. H. Bennett, *Phys. Rev.* **45**, 890 (1934).
- [2] A. S. Bishop, *Project Sherwood* (Addison-Wesley, Reading, MA, 1958).
- [3] W. A. Newcomb, *Ann. Phys. (N.Y.)* **10**, 232 (1960).
- [4] A. A. Ware, *Nucl. Fusion Suppl.* **3**, 869 (1962).
- [5] A. A. Newton, J. Marshall, and R. L. Morse, in *Proceedings of the Third European Conference on Controlled Fusion and Plasma Physics, Utrecht, 1969* (Wolters-Noordhoff, Groningen, 1969), p.119.
- [6] V. G. Belan, S. P. Zolotarev, V. F. Levahov, V. S. Mainashev, A. I. Morozov, V. L. Podkovyrov, and Yu. V. Skvortsov, *Sov. J. Plasma. Phys.* **16**, 96 (1990).
- [7] C. W. Hartman, G. Carlson, M. Hoffman, R. Werner, and D. Y. Cheng, *Nucl. Fusion* **17**, 909 (1977).
- [8] C. W. Hartman, J. L. Eddleman, R. Moir, and U. Shumlak, *Fusion Technol.* **26**, 1203 (1994).
- [9] C. W. Hartman, J. L. Eddleman, A. A. Newton, L. J. Perkins, and U. Shumlak, *Comments Plasma Phys. Control. Fusion* **17**, 267 (1996).
- [10] U. Shumlak and C. W. Hartman, *Phys. Rev. Lett.* **75**, 3285 (1995).
- [11] T. D. Arber and D. F. Howell, *Phys. Plasmas* **3**, 554 (1996).
- [12] R. E. Peterkin, Jr., M. H. Frese, and C. R. Sovinec, *J. Comput. Phys.* **140**, 148 (1998).
- [13] U. Shumlak, T. W. Hussey, and R. E. Peterkin, Jr., *IEEE Trans. Plasma Sci.* **23**, 83 (1995).
- [14] K. F. Schoenberg, R. A. Gerwin, R. W. Moses, Jr., J. T. Scheuer, and H. P. Wagner, *Phys. Plasmas* **5**, 2090 (1998); A. I. Morozov, *Sov. J. Plasma Phys.* **16**, 69 (1990).
- [15] D. J. Den Hartog and R. P. Golingo, *Rev. Sci. Instrum.* **72**, 2224 (2001).